The Drosophila retinoblastoma protein, Rbf1, induces a Debcl-and Drp1-dependent mitochondrial apoptosis

Amandine Clavier, Vincent Ruby, Aurore Rincheval-Arnold, Bernard Mignotte, Isabelle Guenal

© 2015. Published by The Company of Biologists Ltd | Journal of Cell Science (2015) 128, 3239-3249 doi:10.1242/jcs.169896

RESEARCH ARTICLE

The *Drosophila* retinoblastoma protein, Rbf1, induces a *Debcl*- and *Drp1*-dependent mitochondrial apoptosis

Amandine Clavier[1,2], Vincent Ruby[1], Aurore Rincheval-Arnold[1], Bernard Mignotte[1,2] and Isabelle Guénal[1,*]

ABSTRACT

In accordance with its tumor suppressor role, the retinoblastoma protein pRb can ensure pro-apoptotic functions. *Rbf1*, the *Drosophila* homolog of *Rb*, also displays a pro-apoptotic activity in proliferative cells. We have previously shown that the *Rbf1* pro-apoptotic activity depends on its ability to decrease the level of anti-apoptotic proteins such as the Bcl-2 family protein Buffy. Buffy often acts in an opposite manner to Debcl, the other *Drosophila* Bcl-2-family protein. Both proteins can localize at the mitochondrion, but the way they control apoptosis still remains unclear. Here, we demonstrate that *Debcl* and the pro-fission gene *Drp1* are necessary downstream of *Buffy* to trigger a mitochondrial fragmentation during *Rbf1*-induced apoptosis. Interestingly, *Rbf1*-induced apoptosis leads to a *Debcl*- and *Drp1*-dependent reactive oxygen species production, which in turn activates the Jun Kinase pathway to trigger cell death. Moreover, we show that Debcl and Drp1 can interact and that Buffy inhibits this interaction. Notably, Debcl modulates Drp1 mitochondrial localization during apoptosis. These results provide a mechanism by which *Drosophila* Bcl-2 family proteins can control apoptosis, and shed light on a link between Rbf1 and mitochondrial dynamics *in vivo*.

KEY WORDS: Apoptosis, Mitochondrial dynamics, Debcl, Rbf1, Drp1

INTRODUCTION

The retinoblastoma susceptibility gene (*Rb*) is a tumor suppressor gene mutated in a large variety of cancer (Di Fiore et al., 2013). Its tumor suppressive activity is at least partially dependent on its ability to induce cell cycle arrest. However, the role of pRb in cancer is not limited to cell cycle regulation and appears to be more complex. Indeed, pRb can be pro-apoptotic (Bowen et al., 1998; Hilgendorf et al., 2013; Ianari et al., 2009) or anti-apoptotic (Biasoli et al., 2013; Morgenbesser et al., 1994; Tsai et al., 1998), and the regulation of these opposite roles of pRb towards apoptosis remains poorly understood. The ability of pRb to induce apoptosis fits with its tumor suppressor function. Deciphering the molecular mechanisms involved in pRb pro-apoptotic activity could provide important clues for a better understanding of pRb roles in cancer suppression. *Drosophila* allows us to characterize *in vivo* the properties of *Rbf1*, the *Rb* homologue, in the control of apoptosis. As with pRb, Rbf1 can be either pro- or anti-apoptotic depending on the cellular context. For instance, *Rbf1* overexpression leads to apoptosis in proliferating cells but not in post-mitotic cells (Milet et al., 2010). Moreover, we have recently shown that *Rbf1* induces cell death by reducing the expression of the anti-apoptotic Bcl-2 family gene *Buffy* (Clavier et al., 2014) which encodes a mitochondrial protein, suggesting the existence of a mitochondrial death pathway in Rbf1-induced apoptosis.

Mitochondria have a pivotal role in apoptosis regulation in vertebrates (Estaquier et al., 2012; Green et al., 2014; Tait and Green, 2013). Intermembrane space proteins, such as cytochrome *c*, are released in the cytosol to promote caspase activation. This process requires mitochondrial outer membrane permeabilization, which is tightly regulated by Bcl-2 family proteins (Garcia-Sáez, 2012; Hardwick and Soane, 2013). In *Drosophila*, this family contains only two members: *Buffy* (Quinn et al., 2003) and *Death executioner Bcl-2 homologue* (*Debcl*) (Brachmann et al., 2000; Colussi et al., 2000; Igaki et al., 2000; Zhang et al., 2000). Although *Debcl* is not required for most of developmental cell death, it is necessary for apoptosis in specific contexts, such as pruning cells and embryonic cell death (Galindo et al., 2009; Senoo-Matsuda et al., 2005) or DNA-damage-induced apoptosis (Sevrioukov et al., 2007). Moreover, ectopic expression of *Debcl* induces apoptosis (Brachmann et al., 2000; Colussi et al., 2000; Igaki et al., 2000; Zhang et al., 2000). Thus, the mitochondrial protein Debcl displays a pro-apoptotic activity in flies. Buffy can act as an anti-apoptotic protein by physically interacting with Debcl to suppress Debcl-induced cell death (Quinn et al., 2003), whereas *Debcl* is required to inhibit *Buffy* in DNA-damage-induced apoptosis (Sevrioukov et al., 2007). Nevertheless, the mode of action of the *Drosophila* Bcl-2 proteins remains elusive.

Although early studies did not emphasize a crucial role of mitochondria during apoptosis in fly (Dorstyn et al., 2004; Means et al., 2006; Zimmermann et al., 2002), more recent data show that this organelle has a more substantial role. First, key players of *Drosophila* apoptosis are localized to mitochondria, including the caspases Dronc and Drice (Dorstyn et al., 2002) or the pro-apoptotic proteins Reaper (Freel et al., 2008; Olson et al., 2003; Thomenius et al., 2011), Hid (Abdelwahid et al., 2007; Morishita et al., 2013) and Grim (Claveria et al., 2002). For some of these proteins, the loss of mitochondrial localization is associated with a reduction of the pro-apoptotic function (Abdelwahid et al., 2007; Freel et al., 2008; Olson et al., 2003; Sandu et al., 2010). Second, caspases can be activated *in vitro* by mitochondria from apoptotic S2 cells (Varkey et al., 1999), suggesting that some mitochondrial proteins are required for apoptosis. Such proteins include Omi (also known as HtrA2) (Challa et al., 2007) and the *Drosophila* translocator protein (TSPO) (Lin et al., 2014), which are involved in irradiation-induced apoptosis, and cytochrome *c* and *d*, which are necessary for developmental cell death in the eye (Mendes et al., 2006).

Interestingly, an increase in mitochondrial fragmentation can be observed during apoptosis in *Drosophila*. Dynamin-related protein 1 (Drp1), a large GTPase of the dynamin family, is required for mitochondrial fission, whereas the homologue of mitofusin 2,

[1]Université de Versailles Saint-Quentin-en-Yvelines, Laboratoire de Génétique et Biologie Cellulaire, EA4589, 2 avenue de la Source de la Bièvre, Montigny-le-Bretonneux 78180, France. [2]Ecole Pratique des Hautes Etudes, Laboratoire de Génétique et Biologie Cellulaire, 2 avenue de la Source de la Bièvre, Montigny-le-Bretonneux 78180, France.

*Author for correspondence (isabelle.guenal@uvsq.fr)

Received 6 February 2015; Accepted 10 July 2015

Journal of Cell Science (2015) 128, 3239-3249 doi:10.1242/jcs.169896

Mitochondrial assembly regulatory factor (Marf) and Optic atrophy 1 (Opa1) are respectively required for outer and inner mitochondrial membrane fusion. Knockdown of *Drp1* using genetic mutants or RNA interference (RNAi) leads to apoptosis inhibition (Abdelwahid et al., 2007; Goyal et al., 2007), highlighting the role of mitochondrial dynamics in fly cell death. Interestingly, recent data indicate that Reaper induces mitochondrial fragmentation by binding and inhibiting the pro-fusion protein Marf. This decrease in mitochondrial fusion allows caspase activation and eventually apoptosis (Thomenius et al., 2011). However, the precise mechanisms involved in the *Drosophila* mitochondrial cell death pathway remain to be uncovered. For example, a potential link between Bcl-2 family proteins and mitochondrial fission remains to be elucidated.

In this study, we used Rbf1-induced apoptosis to highlight the role of Bcl-2 family genes in *Drosophila* apoptosis and display a new aspect of Rbf1 pro-apoptotic activity. We show that Debcl is required downstream of *Buffy* in Rbf1-induced apoptosis. Debcl induces mitochondrial fragmentation by binding the pro-fission protein Drp1, which triggers the production of mitochondrial reactive oxygen species (ROS), thereby activating the c-Jun N-terminal kinase (JNK) pathway and eventually leading to cell death.

RESULTS

Debcl is required downstream of *Buffy* for Rbf1-induced apoptosis

We have previously shown that the Bcl-2 anti-apoptotic gene *Buffy* counteracts Rbf1-induced apoptosis (Clavier et al., 2014). To determine whether *Debcl*, the second *Bcl-2* gene in *Drosophila*, is involved in Rbf1-induced apoptosis, we performed genetic interaction tests. As previously shown, *Rbf1* overexpression at the dorso-ventral frontier of wing imaginal discs using the UAS-Gal4 system with the *vestigial* (*vg*) Gal4 driver induced notches along the wing margin. The number of notches correlates with the amount of apoptosis in wing imaginal discs of third-instar larvae (Milet et al., 2010). Wing phenotypes were classified into four categories according to the number of notches: wild type (no notch), weak, intermediate and strong (Fig. 1A). When *Rbf1* was overexpressed in a heterozygous background for the loss-of-function mutant $Debcl^{E26}$, a significant shift of the distribution toward weaker phenotypes was observed as compared to overexpression of *Rbf1* only (Fig. 1B), showing that *Debcl* participates in the notched wing phenotype induced by Rbf1. TUNEL staining quantification of third-instar larval wing imaginal discs confirmed that the shift of phenotypic distribution was related to variation in the amount of apoptosis in larvae. Indeed, many cells were TUNEL-labeled in *vg-Gal4/+; UAS-Rbf1/+* wing discs but we observed a significant decrease in the TUNEL-labeled cell percentage when *Rbf1* was overexpressed in a $Debcl^{E26}$ background (Fig. 1C). These results indicate that Debcl has a pivotal role in Rbf1-induced apoptosis.

Because Rbf1 transcriptionally represses *Buffy*, we hypothesized that *Buffy* inhibition might indirectly activate Debcl in Rbf1-induced apoptosis. To determine the epistatic relationship between *Buffy* and *Debcl* in Rbf1-induced apoptosis, we performed genetic interaction tests. When *Rbf1* was overexpressed in a $Buffy^{H37}$ loss of function heterozygous background, distribution of the phenotypes significantly shifted toward stronger phenotypes as compared to expression of *Rbf1* alone (Fig. 1B). Interestingly, in a $Debcl^{E26}$ heterozygous background, $Buffy^{H37}$ loss of function could not anymore induce a phenotypic aggravation (*vg-gal4/*$Debcl^{E26}$*; UAS-Rbf1/+* compared with *vg-gal4/*$Debcl^{E26}$ $Buffy^{H37}$*; UAS-Rbf1/+*; Wilcoxon test, n=343, $\alpha=1.6\times10^{-3}$, Ws=3.2). Thus, *Buffy* needs *Debcl* to counteract Rbf1-induced loss of tissue. Similar results were obtained in $Debcl^{E26}$ and $Buffy^{H37}$ homozygous backgrounds (supplementary material Fig. S1). Consistent with these results, the number of apoptotic cells was not significantly different

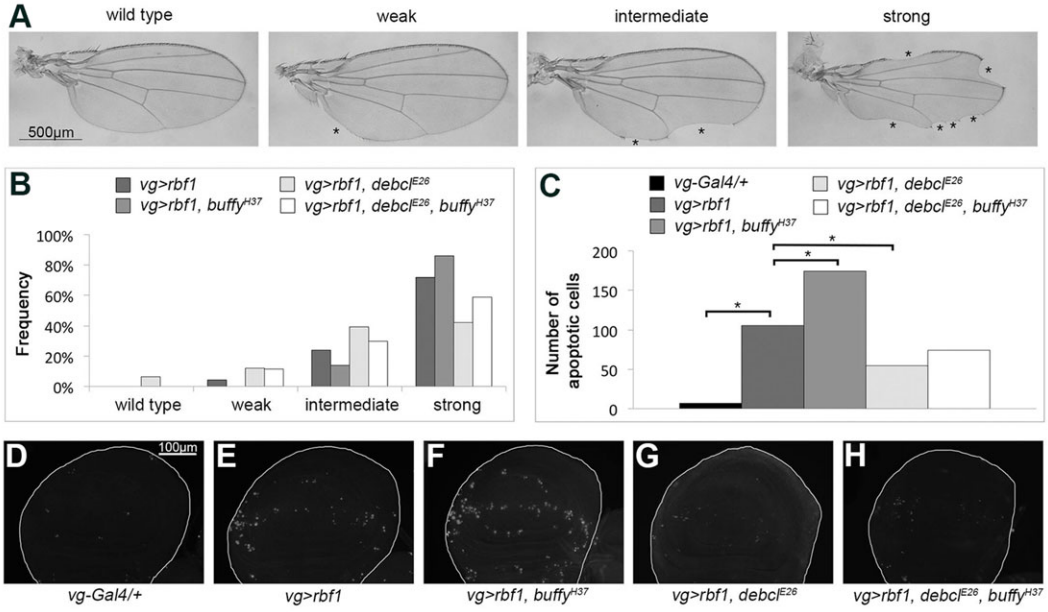

Fig. 1. Rbf1-induced *Debcl*-dependent apoptosis. (A) Fly wings are classified into four categories (wild-type, weak, intermediate and strong) according to the number of notches observed on their margin (asterisks) (Clavier et al., 2014). (B) Distribution of notch wing phenotypes in (1) *vg-Gal4/+;UAS-Rbf1/+*; (2) *vg-Gal4/*$Buffy^{H37}$*;UAS-Rbf1/+*; (3) *vg-Gal4/*$Debcl^{E26}$*;UAS-Rbf1/+* and (4) *vg-Gal4/*$Buffy^{H37}$*,* $Debcl^{E26}$*;UAS-Rbf1/+*. Statistical analysis was performed using Wilcoxon tests: $Debcl^{E26}$, n=305, $\alpha=4.25\times10^{-8}$, Ws=−5.56; $Buffy^{H37}$, n=349, $\alpha=6.53\times10^{-4}$, Ws=3.40; $Debcl^{E26}$, $Buffy^{H37}$, n=364, $\alpha=4.63\times10^{-3}$, Ws=−2.82. Each experiment was independently performed three times. A representative experiment is shown. (C) Quantification of apoptotic cells in the wing imaginal discs pouch visualized by TUNEL staining from the genotypes described previously. Asterisks indicate a statistically significant difference between two genotypes (Student's *t*-test, $\alpha<0.05$). (D–H) Apoptotic cells were visualized by TUNEL staining (white dots) of wing imaginal discs of the genotype indicated at the bottom of the image.

Journal of Cell Science (2015) 128, 3239-3249 doi:10.1242/jcs.169896

between these two genetic backgrounds (Fig. 1C–H). Therefore, *Debcl* is required downstream of *Buffy* in Rbf1-induced apoptosis.

Rbf1 overexpression triggers mitochondrial ROS production in a *Debcl*-dependent manner

We have previously shown that the JNK pathway activation is required to trigger apoptosis in response to *Rbf1* overexpression (Milet et al., 2014). To determine the importance of Debcl in the JNK pathway activation, we quantified the mRNAs of two target genes of the JNK signaling pathway, *mmp1* and *puc*, by quantitative real-time PCR (qRT-PCR). When *Rbf1* was overexpressed under *vg* control, both *mmp1* and *puc* mRNA levels were significantly increased as compared with the vg-Gal4/+ control (Fig. 2A). Consistent with this, when *Rbf1* was overexpressed with *RNAi-hep* in order to decrease *hep* expression, the amount of *mmp1* and *puc* mRNAs was similar to the amount observed for the *vg-Gal4/+* control. These data confirm that Rbf1 induces JNK pathway activation. When *Rbf1* was overexpressed in a $Debcl^{E26}$ heterozygous background (Fig. 2A), *puc* and *mmp1* mRNA levels decreased compared to overexpression of *Rbf1* in a wild-type background. An immunostaining against Mmp1 in these different genetic backgrounds confirmed these data (supplementary material Fig. S2A–D). Thus *Debcl* is required for Rbf1-induced JNK pathway activation in wing imaginal discs.

The JNK pathway can be activated by a wide variety of stimuli, such as receptor–ligand interactions or cellular stresses. In particular, ROS have been reported to activate the JNK pathway (Son et al., 2013). Interestingly, Debcl is localized in mitochondria, which are known to be the major site of ROS production in cells. Therefore, we asked whether *Rbf1* overexpression induces mitochondrial ROS production, which could be responsible for JNK pathway activation. We measured mitochondrial superoxide production with MitoSOX fluorescence by flow cytometry. *Rbf1* overexpression increased the percentage of MitoSOX-positive cells as compared to the *vg-gal4/+* control (Fig. 2B). Superoxide dismutase 2 (Sod2) is a mitochondrial antioxidant enzyme which detoxifies superoxide. Consistent with this, when *Rbf1* and *Sod2* were co-overexpressed, the percentage of MitoSOX-positive cells decreased when compared to overexpression of *Rbf1* alone. We also observed a significant decrease in MitoSOX-positive cells when *Rbf1* was overexpressed in a $Debcl^{E26}$ heterozygous background, thus indicating that *Debcl* is required for Rbf1-induced ROS production. Then, we assessed *GstD1* expression, which is a marker of mitochondrial oxidative stress, in these different genetic backgrounds. An increase in *GstD1* mRNA levels was observed when *Rbf1* was overexpressed in a wild-type background (supplementary material Fig. S2E). By contrast, *Rbf1* overexpression in a $Debcl^{E26}$ heterozygous background did not affect the level of *GstD1* mRNA when compared to the control (supplementary material Fig. S2E). All these data confirm that Rbf1 triggers ROS production in a Debcl-dependent manner. In order to precisely identify the implication of ROS in Rbf1-induced apoptosis, we studied the impact of modifying ROS levels on the adult phenotypes observed in a context of *Rbf1* expression. We used a $Sod2^{\Delta 02}$ loss-of-function mutant and flies overexpressing *Sod2*. When *Rbf1* was overexpressed in a $Sod2^{\Delta 02}$ heterozygous background, the distribution of the wing phenotypes shifted towards stronger phenotypes as compared to overexpression of *Rbf1* alone (Fig. 2C). Conversely, when *Rbf1* and *Sod2* were co-overexpressed, the distribution of wings shifted towards weaker phenotypes. The variation of the phenotypic distribution between these different genetic backgrounds correlated with the variation of apoptotic cell numbers in wing imaginal discs (Fig. 2D). Thus, Sod2 limits Rbf1-induced apoptosis, which suggests that ROS mediate this cell death.

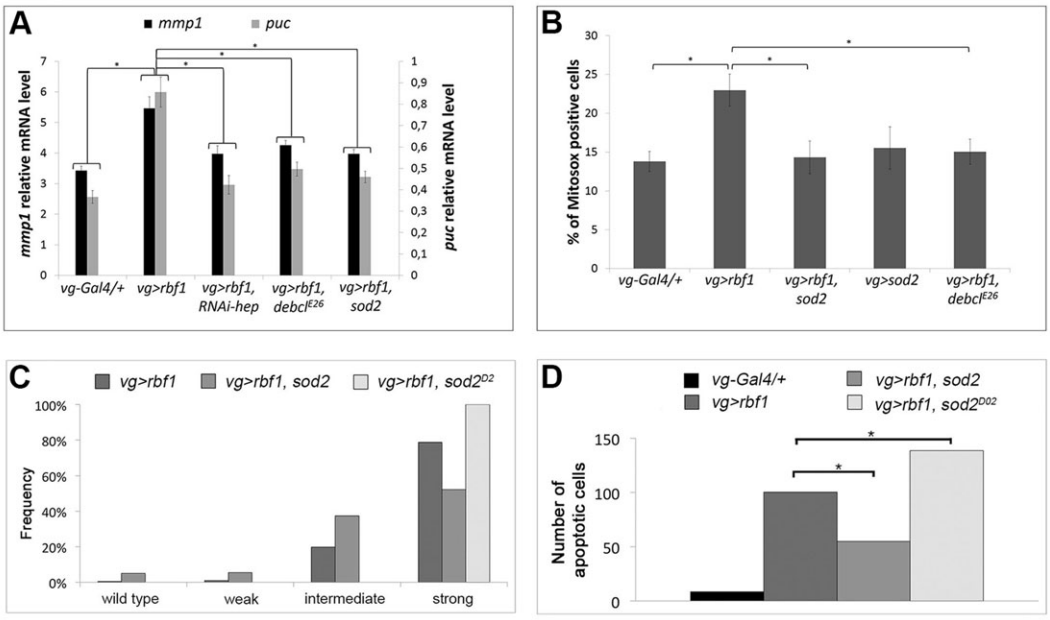

Fig. 2. Rbf1 triggers ROS-dependent JNK activation and apoptosis. (A) Quantification of *mmp1* and *puc* mRNA levels by qRT-PCR on wing imaginal discs from (1) *vg-Gal4/+*, (2) *vg-Gal4/+; UAS-Rbf1/+*, (3) *vg-Gal4/+; UAS-Rbf1/UAS-RNAi-hep*, (4) *vg-Gal4/*$Debcl^{E26}$*; UAS-Rbf1/+* and (5) *vg-Gal4/UAS-Sod2; UAS-Rbf1/+* larvae. (B) Quantification by flow cytometry of MitoSOx staining (a mitochondrial superoxide indicator) in wing imaginal discs from (1) *en-Gal4/+*; (2) *en-Gal4/+;UAS-Rbf1/+*; (3) *en-Gal4/UAS-Sod2;UAS-Rbf1/+*; (4) *en-Gal4/UAS-Sod2* and (5) *en-Gal4/*$Debcl^{E26}$*;UAS-Rbf1/+* larvae. (C) Distribution of notched wing phenotypes in (1) *vg-Gal4/+;UAS-Rbf1/+*, (2) *vg-Gal4/UAS-Sod2;UAS-Rbf1/+* and (3) *vg-Gal4/*$Sod2^{\Delta 02}$*;UAS-Rbf1/+*. Statistical analysis was performed using Wilcoxon tests: *Sod2*, n=423, $\alpha=3.37\times10^{-9}$, Ws=−6.03; $Sod2^{\Delta 02}$, n=269, $\alpha=5.3.10^{-4}$, Ws=3.46. Each experiment was independently performed three times. A representative experiment is shown. (D) Quantification of apoptotic cells visualized by TUNEL staining in wing imaginal discs from the previously described genotypes. Error bars are the s.e.m. Asterisks indicate a statistically significant difference between two genotypes (Student's *t*-test, $\alpha<0.05$).

Journal of Cell Science

Journal of Cell Science (2015) 128, 3239-3249 doi:10.1242/jcs.169896

We then wondered whether ROS are involved in JNK pathway activation, which could explain their role in Rbf1-induced cell death. When *Rbf1* and *Sod2* were co-overexpressed, Mmp1 protein (supplementary material Fig. S2D) and mRNA levels (Fig. 2A) decreased when compared to overexpression of *Rbf1* alone. Hence, Sod2 inhibits Rbf1-induced JNK pathway activation, which suggests that ROS are required to activate this signaling pathway. Taken together, these data show that *Rbf1* overexpression induces a *Debcl*-dependent mitochondrial ROS production, thereby leading to JNK pathway activation and finally to cell death.

Rbf1 induces mitochondrial fragmentation which is required for ROS production and cell death

Mitochondrial fission, which can occur during apoptosis in mammalians and *Drosophila* cells (Desagher and Martinou, 2000; Goyal et al., 2007), can regulate ROS generation (Park et al., 2013; Qi et al., 2013). Interestingly, apoptosis can be blocked with a dominant-negative mutation or specific RNAi-mediated knockdown of the pro-fission gene *Drp1* (Abdelwahid et al., 2007; Arnoult et al., 2005; Breckenridge et al., 2003; Frank et al., 2001). Several studies have highlighted the role of Bcl-2 family proteins in the control of mitochondrial dynamics during apoptosis in mammalian cells (Brooks et al., 2007; Frank et al., 2001; Karbowski et al., 2004, 2002; Rolland and Conradt, 2010; Sheridan et al., 2008; Wasiak et al., 2007). Therefore, we assessed the impact of *Rbf1* overexpression on mitochondrial dynamics. To visualize the mitochondrial network, we used a Streptavidin Alexa Fluor® 488 conjugate. As expected, *vg-Gal4/+* control disc cells had a typical filamentous mitochondrial network (Fig. 3A), whereas we observed punctuate units in response to *Rbf1* overexpression (Fig. 3B). This punctiform staining is a hallmark of mitochondrial fragmentation. Of note, when *Rbf1* was overexpressed in a $Drp1^{KG03815}$ heterozygous loss-of-function background (Fig. 3D), the mitochondrial network appeared more filamentous than when *Rbf1* was overexpressed alone. These data suggest that Rbf1-induced mitochondrial fragmentation is due to an increase in mitochondrial fission that involves Drp1. Interestingly, we also observed a rescue of this fragmentation when *Rbf1* was overexpressed in a $Debcl^{E26}$ heterozygous background (Fig. 3E) or when *Rbf1* and *Buffy* were co-overexpressed (Fig. 3F). Thus, Debcl is required for Rbf1-induced mitochondrial fission, whereas Buffy prevents this fragmentation.

We used the $Drp1^{KG03815}$ loss-of-function mutation to determine the implication of mitochondrial fission in Rbf1-induced apoptosis. When *Rbf1* was overexpressed in a $Drp1^{KG03815}$ heterozygous background, we observed a decrease in wing notches as well as a decrease in the number of apoptotic cells in wing imaginal discs (Fig. 3G,H) compared to *Rbf1* overexpression alone. Thus, Drp1 is required for Rbf1-induced apoptosis and this suggests that mitochondrial fission plays a key role in Rbf1-induced cell death.

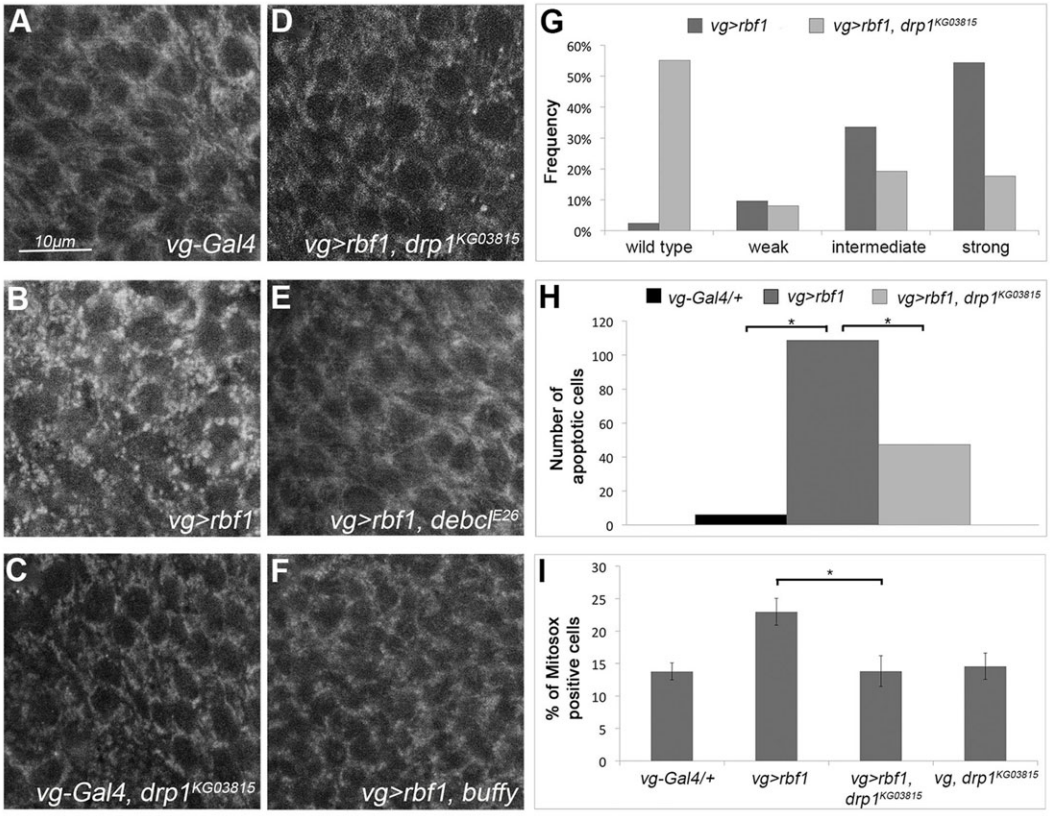

Fig. 3. Rbf1-induced apoptosis requires Drp1-mediated mitochondrial fission. (A–F) Mitochondrial morphology was observed by Alexa-Fluor-488-coupled streptavidin in wing imaginal discs from *vg-Gal4/+* (A); *vg-Gal4/+;UAS-Rbf1/+* (B); *vg-Gal4/*$Drp1^{KG03815}$ (C); *vg-Gal4/*$Drp1^{KG03815}$*;UAS-Rbf1/+* (D); *vg-Gal4/*$Debcl^{E26}$*; UAS-Rbf1/+* (E); and *vg-Gal4/UAS-Buffy ;UAS-Rbf1/+* (F) larvae. Scale bar: 10 µm. (G) Distribution of notch wing phenotypes in *vg-Gal4/+;UAS-Rbf1/+* and *vg-Gal4/*$Drp1^{KG03815}$*;UAS-Rbf1/+*. n=312, $\alpha<10^{-30}$ and Ws=−9.52. Each experiment was independently performed three times. A representative experiment is shown. (H) Quantification of apoptotic cells visualized by TUNEL staining of wing imaginal discs from (1) *vg-Gal4/+*; (2) *vg-Gal4/+;UAS-Rbf1/+* and (3) *vg-Gal4/*$Drp1^{KG03815}$*;UAS-Rbf1/+* flies. (I) Quantification by flow cytometry of MitoSOx staining (a mitochondrial superoxide indicator) in wing imaginal discs from *vg-Gal4/+*; *vg-Gal4/+;UAS-Rbf1/+;* *vg-Gal4/*$Drp1^{KG03815}$*;UAS-Rbf1/+* and *vg-Gal4/*$Drp1^{KG03815}$ larvae. Error bars are the s.e.m. Asterisks indicate a significant difference between two genotypes (Student's t-test, $\alpha<0.05$).

Journal of Cell Science (2015) 128, 3239-3249 doi:10.1242/jcs.169896

In addition, we observed a significant decrease in the proportion of Mitosox-positive cells when *Rbf1* was overexpressed in a *Drp1*^{KG03815} heterozygous background (Fig. 3I) compared to overexpression of *Rbf1* alone, indicating that Drp1 is required for Rbf1-induced ROS production. Furthermore, we verified that *Drp1* loss of function decreased Rbf1-induced JNK pathway activation (supplementary material Fig. S3). Taken together, these results show that *Rbf1* overexpression induces a *Debcl*- and *Drp1*-dependent mitochondrial fragmentation that promotes ROS production, JNK pathway activation and eventually cell death.

Debcl induces mitochondrial fragmentation to trigger ROS production and cell death

Our data indicate that Debcl plays a key role in Rbf1-induced apoptosis. We assessed whether the cascade of events (mitochondrial fragmentation, ROS production and JNK pathway activation) characterized in Rbf1-induced apoptosis occurs in a similar fashion in Debcl-induced apoptosis. Indeed, Debcl has been previously described as a pro-apoptotic protein. For instance, overexpression of *Debcl* using the UAS-Gal4 system with the *patched*-Gal4 (*ptc-Gal4*) driver induces apoptosis along the antero-posterior frontier (Colin et al., 2014). To determine whether Debcl-induced apoptosis is associated with an altered mitochondrial network, we used a Streptavidin Alexa Fluor® 488 conjugate.

In *ptc-Gal4/+* control discs, the mitochondrial network was filamentous, whereas punctuated staining appeared in response to *Debcl* overexpression (Fig. 4A,B). Thus, Debcl, as Rbf1 does, induces a mitochondrial fragmentation in wing discs. When *Debcl* was overexpressed in a loss-of-function *Drp1*^{KG03815} heterozygous background (Fig. 4C), the mitochondrial network appeared more filamentous than when *Debcl* was overexpressed in a wild-type background. These data suggest that Debcl-induced mitochondrial fragmentation results from an increase in mitochondrial fission.

We performed genetic interaction tests between *Debcl* and *Drp1*^{KG03815} loss of function to determine the implication of mitochondrial fission in Debcl-induced apoptosis. In the adult wing,

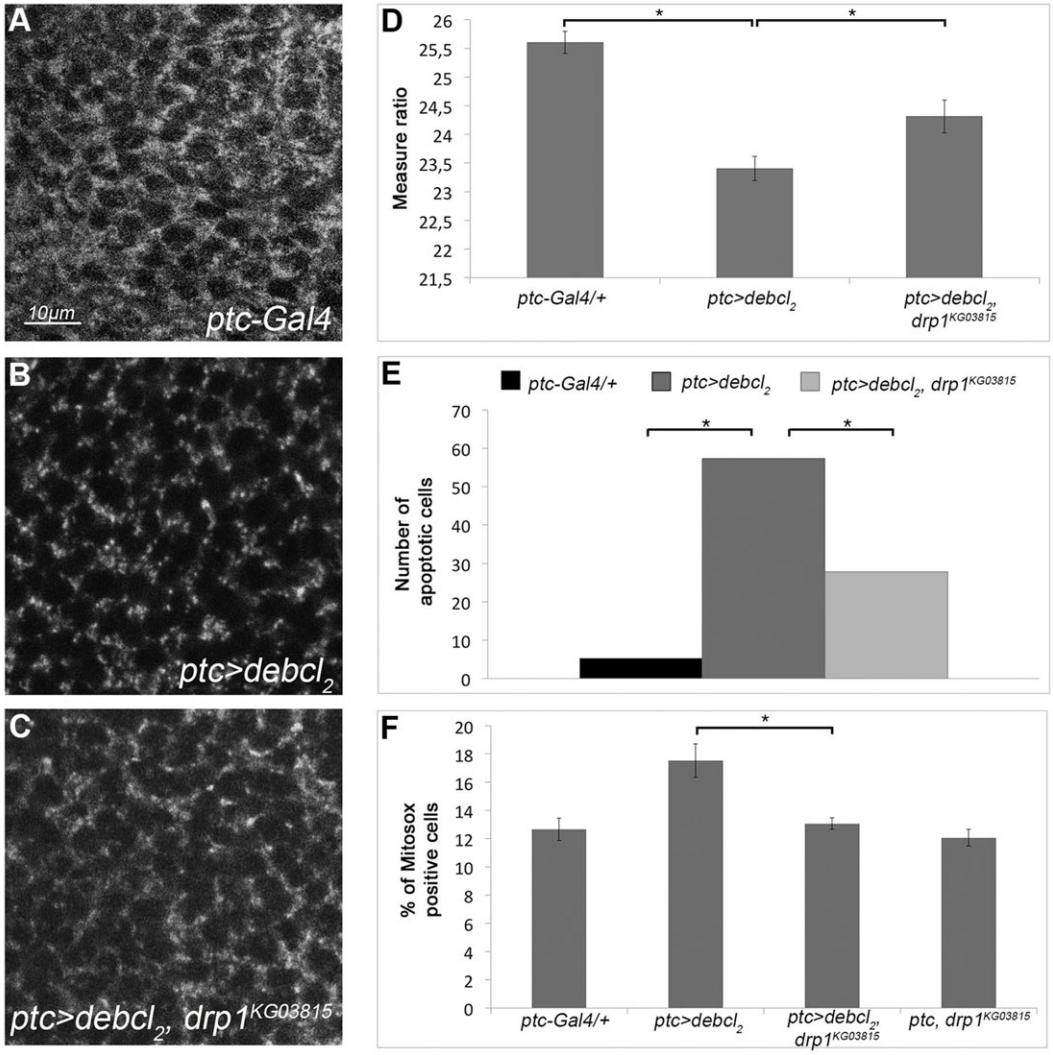

Fig. 4. Debcl-induced apoptosis requires Drp1 mediated mitochondrial fission. (A–C) Mitochondrial morphology observed by Alexa-Fluor-488-coupled streptavidin in wing imaginal discs from *ptc-Gal4/+* (A); *ptc-Gal4,UAS-Debcl/+;UAS-Debcl/+* (B) and *vg-Gal4,UAS-Debcl/Drp1*^{KG03815}*;UAS-Debcl/+* (C) larvae. Scale bar: 10 µm. (D) Measure of relative distance between the L3 and L4 veins of the previously described genotypes. (E) Quantification of apoptotic cells visualized by TUNEL staining of wing imaginal discs from the previously described genotypes. (F) Quantification by flow cytometry of MitoSOx staining (a mitochondrial superoxide indicator) in wing imaginal discs from *ptc-Gal4/+*; *ptc-Gal4/+;UAS-Rbf1/+*; *ptc-Gal4/Drp1*^{KG03815}*;UAS-Rbf1/+* and *ptc-Gal4/Drp1*^{KG03815} larvae. Error bars are the s.e.m. Asterisks indicate a significant difference between two genotypes (Student's *t*-test, α<0.05).

Journal of Cell Science (2015) 128, 3239-3249 doi:10.1242/jcs.169896

this apoptosis led to a decrease in the distance between veins L3 and L4 (Fig. 4D; Colin et al., 2014). When *Debcl* was overexpressed in a $Drp1^{KG03815}$ heterozygous background, we observed a rescue of the wing loss of tissue (Fig. 4D) as well as a decrease in the amount of apoptosis in wing imaginal discs (Fig. 4E) as compared to overexpression of *Debcl* in a wild-type background. Thus, Drp1 is required for Debcl-induced apoptosis, which suggests that mitochondrial fission plays a key role in Debcl-induced cell death.

We then investigated whether *Debcl* overexpression was sufficient to induce mitochondrial ROS production. Indeed, *Debcl* overexpression increases the proportion of Mitosox-positive cells in the wing imaginal discs, when compared to the *ptc-gal4/+* control (Fig. 4F). In addition, we observed a significant decrease in the percentage of Mitosox-positive cells when *Debcl* was overexpressed in a $Drp1^{KG03815}$ heterozygous background when compared to a wild-type background, indicating that Drp1 is required for Debcl-induced ROS production.

These results highlight that *Debcl* overexpression induces a *Drp1*-dependent mitochondrial fragmentation leading to ROS production and thus to cell death. Therefore, *Debcl* overexpression is sufficient to recapitulate the mitochondrial events induced by Rbf1.

Debcl physically interacts with Drp1 *in vivo*

Drp1 plays a key role both in Rbf1- and Debcl-induced apoptosis. In mammals, in the absence of apoptotic stimuli, Drp1 is mostly cytosolic, whereas it becomes stabilized when it is bound to mitochondria in apoptotic cells (Wasiak et al., 2007). Because Debcl is a mitochondrial protein, we wondered whether Drp1 and Debcl physically interact during apoptosis. We used transgenic larvae expressing Debcl–HA and/or FLAG–HA–Drp1 to perform immunoprecipitations with an anti-FLAG antibody. When FLAG–HA–Drp1 was immunoprecipitated, we observed a co-immunoprecipitation of Debcl–HA (Fig. 5A), suggesting that Drp1 and Debcl physically interact *in vivo*. By contrast, the innocuous mitochondrial protein Tom40 did not co-immunoprecipitate, proving the specificity of Debcl and Drp1 interaction. Interestingly, when *Buffy* was overexpressed, the co-immunoprecipitation of Debcl–HA was lost (Fig. 5A), suggesting that Buffy inhibits the physical interaction between Debcl and Drp1. We assessed the occurrence of this physical interaction *in vivo* by using a proximity ligation *in situ* assay (Fig. 5B). White dots are specifically observed in the *ptc* domain when *Debcl* is overexpressed, indicating that Debcl and Drp1 colocalize within 40 nm. This approach confirmed that the two proteins can interact together *in vivo*. Because we do not have antibodies against Debcl, we were unable to test whether this interaction occurs during Rbf1-induced apoptosis without *Debcl–HA* overexpression. Nevertheless, we observed a significant increase in FLAG–HA–Drp1 proteins in the mitochondrial-enriched fraction when *Rbf1* was overexpressed compared to upon expression of the *vg-Gal4*, *FLAG-HA-Drp1* control (Fig. 5C,D). Consistent with this, the quantity of FLAG–HA–Drp1 significantly decreased in the cytosolic fraction. Interestingly, $Debcl^{E26}$ heterozygous loss of function impeded both Drp1 mitochondrial accumulation and Drp1 cytosolic depletion (Fig. 5C,D). This result indicates that Debcl is required for Drp1 mitochondrial enrichment and argues for an interaction between Debcl and Drp1 during Rbf1-induced apoptosis.

Taken together, these results indicate that Debcl and Drp1 are part of the same protein complex. This complex formation facilitates Drp1 mitochondrial localization which might trigger the mitochondrial fragmentation observed following *Debcl* or *Rbf1* overexpression.

DISCUSSION

In this paper, we characterized the death pathway induced by Rbf1 in *Drosophila* (Fig. 6) and highlighted the role of Bcl-2 family genes during this process. Although Debcl displays a pro-apoptotic activity in different tissues (Brachmann et al., 2000; Colussi et al., 2000; Igaki et al., 2000; Senoo-Matsuda et al., 2005), its mechanism of action was practically unknown. Our results show that *Debcl* is required for Rbf1-induced mitochondrial fragmentation, ROS production and JNK pathway activation, which leads to Rbf1-induced apoptosis. Moreover, *Debcl* overexpression can recapitulate by itself these different events initiated at the mitochondria level. Thus, our work sheds light on the molecular mechanisms involved in Debcl pro-apoptotic activity. In addition, our results corroborate previous data (Quinn et al., 2003; Sevrioukov et al., 2007) indicating that Debcl and Buffy act in opposing ways. Indeed, we show that *Buffy* loss of function leads to an increase in Rbf1-induced apoptosis only in a *Debcl* loss-of-function background.

During Rbf1-induced apoptosis, the mitochondrial network is fragmented. Rbf1-induced mitochondrial fragmentation and cell death depend on *Drp1*. Thus our data suggest that Rbf1 triggers mitochondrial fission, which in turns induces cell death. However, we have not fully shown that Drp1 pro-apoptotic activity relies on its capacity to induce mitochondrial fission. Of note, other data support this idea. Indeed, blocking mitochondrial fusion in wing imaginal discs with an RNAi directed against *marf* causes apoptosis (Thomenius et al., 2011). Moreover, Thomenius et al. have demonstrated that Reaper induces mitochondrial fragmentation by binding to and inhibiting Marf, which in turn leads to caspase activation and cell death (Thomenius et al., 2011). Thus a growing number of studies point out the importance of mitochondrial dynamics in apoptosis regulation. Because Drp1 is involved in Rbf1-induced mitochondrial ROS production, it is conceivable that Rbf1-induced mitochondrial fragmentation affects the mitochondrial respiratory chain function and increases the electron leakage, which could explain the increase in mitochondrial ROS production. In this case, the role of Drp1 in cell death would be closely related to its function in mitochondrial fission.

A number of studies on mammals support the link between pro-apoptotic Bcl-2 proteins and the mitochondrial fusion and fission machinery (Rolland and Conradt, 2010). During apoptosis, mitochondrial fragmentation occurs simultaneously with Bax relocation to mitochondria. Bax colocalizes with Drp1 and Mitofusin 2 at fission sites (Karbowski et al., 2002). Bax plays a crucial role in mitochondrial fragmentation during apoptosis (Brooks et al., 2007; Frank et al., 2001). By contrast, Mitofusin2 opposes Bax-induced apoptosis (Neuspiel et al., 2005). Thus pro-apoptotic Bcl-2 proteins cause mitochondrial fragmentation by activating fission and/or blocking fusion. Here, we show for the first time in *Drosophila*, that Debcl and Buffy control mitochondrial dynamics to regulate cell death induction. Indeed, we show that Debcl is required for the mitochondrial fragmentation observed during *Rbf1*-induced apoptosis. Galindo et al. have shown that mitochondrial morphology remains unaffected by *Debcl* loss of function (Galindo et al., 2009). Taken together, these results indicate that Debcl has a role in mitochondrial dynamics, but only in specific contexts such as in apoptotic conditions. Interestingly, Debcl also modulates mitochondrial density and activity, independently of apoptosis, in neuronal processes (Tsubouchi et al., 2009). The role of Debcl in mitochondrial dynamics during apoptosis involves a physical interaction between Debcl and Drp1. This interaction might be responsible for Drp1 activation and

Journal of Cell Science (2015) 128, 3239-3249 doi:10.1242/jcs.169896

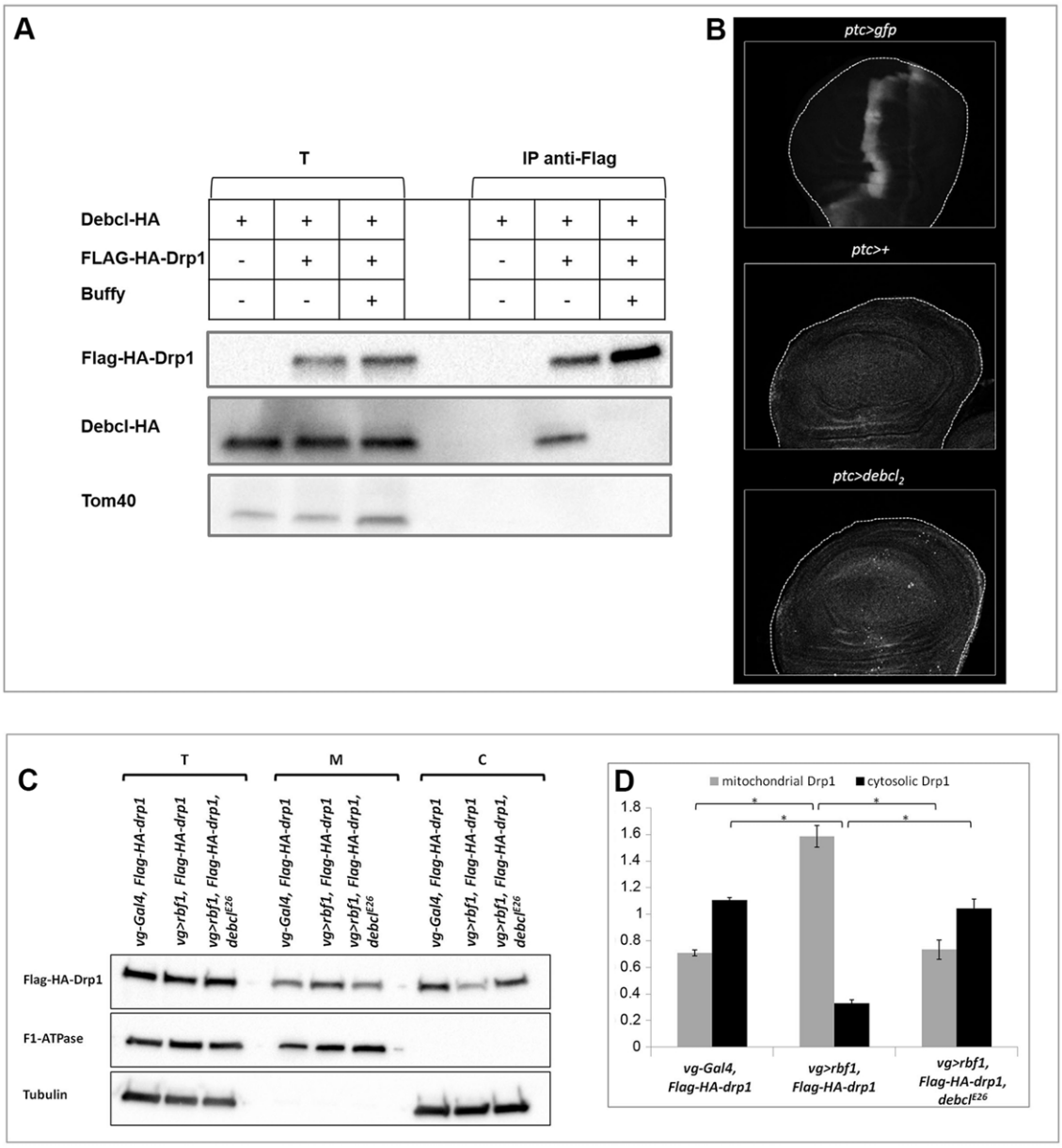

Fig. 5. Debcl physically interacts with Drp1. (A) Immunoprecipitation assays were performed with an anti-Flag antibody on cell extracts from (1) *ptc-Gal4/+; UAS-Debcl-HA/+*; (2) *ptc-Gal4/+;UAS-Debcl-HA/FLAG-HA-Drp1* and (3) *ptc-Gal4/UAS-Buffy;UAS-Debcl-HA/FLAG-HA-Drp1* larvae. Western blotting on total extract (T) and immunoprecipitates (IP) were analyzed with anti-Flag (Drp1), anti-HA (Debcl) or anti-TOM40 antibodies. (B) Duolink® staining (white dots) against Drp1 and Debcl–HA in wing imaginal discs from *ptc-Gal4/+* and *ptc-Gal4,UAS-Debcl-HA/+; UAS-Debcl-HA/+* larvae. The control for expression domain of *ptc* is *ptc-Gal4/+; UAS-eGFP/+* (top). All discs are shown with posterior to the left. (C) Cell fractionation was performed on cell extracts from (1) *vg-Gal4/+;FLAG-HA-Drp1/+*; (2) *vg-Gal4/+;UAS-Rbf1/FLAG-HA-Drp1* and (3) *vg-Gal4/Debcl^{E26};UAS-Rbf1/FLAG-HA-Drp1* larvae. Total extract (T), the mitochondrial fraction (M) and the cytosolic fraction (C) were subjected to immunoblot analysis with anti-HA (Drp1), anti-F1-ATPase (β subunit) and anti-Tubulin antibodies. (D) Quantification of the immunoblot staining against FLAG-HA-Drp1 presented in C. Error bars are the s.e.m. Asterisks indicate a significant difference between two genotypes (Student's *t*-test, α<0.05).

therefore for mitochondrial fission. There is no evidence for a physical interaction between Drp1 and a pro-apoptotic member of Bcl-2 family in mammals. However, Bax participates in Drp1 activation by other means. During apoptosis, Bax stimulates Drp1 sumoylation and thus promotes the stable association of Drp1 to mitochondrial membranes. Moreover, outer mitochondrial membrane permeabilization mediated by Bax allows the release of DDP (also known as TIMM8a). This protein physically interacts with Drp1 (Arnoult et al., 2005), which stabilizes Drp1 at mitochondria where it can induce mitochondrial fragmentation.

Our study also provides a better definition of Rbf1 pro-apoptotic activity. Indeed, our results indicate that Rbf1 can activate Debcl through a transcriptional regulation of *Buffy*. This regulation plays a crucial role in cell death commitment. In mammals, regulation of Bcl-2 family proteins by pRb are usually transcriptional regulations mediated by pRb and E2F (Bertin-Ciftci et al., 2013; Bracken et al., 2004; Hao et al., 2007; Hershko and Ginsberg, 2004; Morales et al., 2011; Zhao et al., 2005). However, a recent study has demonstrated that pRb induces apoptosis directly at the mitochondria where pRb binds and conformationally activates Bax (Hilgendorf et al., 2013). Thus, the role

Journal of Cell Science

Journal of Cell Science (2015) 128, 3239-3249 doi:10.1242/jcs.169896

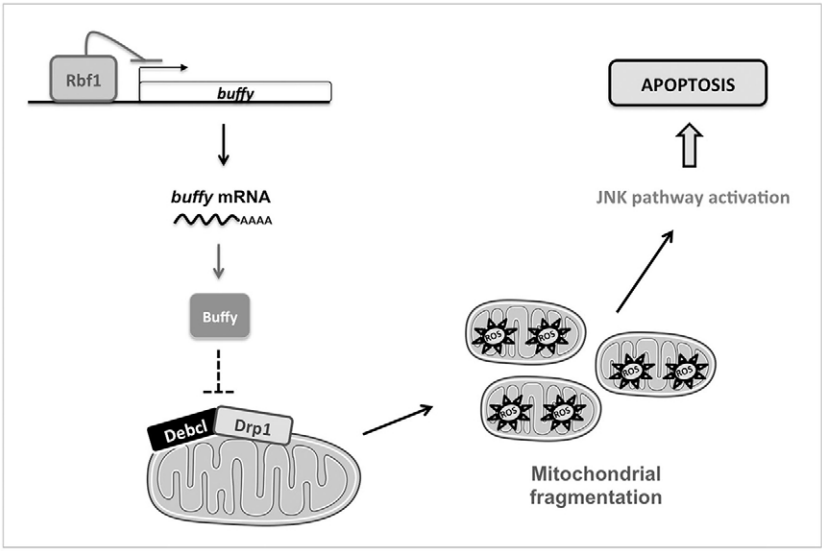

Fig. 6. Rbf1 triggers apoptosis through mitochondrial events in a Debcl-dependent fashion. Rbf1 inhibits *Buffy* expression. The decrease in Buffy level results in Debcl activation. Thus, Debcl interacts with Drp1 at mitochondria, which leads to mitochondrial fragmentation. Drp1 and Debcl trigger a ROS production that activates apoptosis through the JNK pathway.

of the Bcl-2 family in the control of apoptosis by pRb seems to be conserved between species although operating in different ways.

Our data indicate that *Rbf1* overexpression induces a mitochondrial death pathway involving mitochondrial fragmentation and ROS production in a *Debcl*-dependent manner. Interestingly a role of the Rbf1 and *Drosophila* E2F (dE2F) pathway in the regulation of mitochondrial function has been reported (Ambrus et al., 2013). Indeed Rbf1 and dE2F control the expression of genes encoding mitochondrial proteins. This regulation is crucial for normal induction of apoptosis in response to irradiation. In mammals, pRb at mitochondria activates Bax and mitochondrial apoptosis in response to diverse stimuli (Hilgendorf et al., 2013), which is in agreement with the role of pRb as a tumor suppressor. Thus mitochondria seem to play an important role in the death process induced by Rbf1 or its counterpart pRb. Our data highlight an important role for Drp1 in Rbf1-induced apoptosis. In mammals, some data indicate that Bax and Drp1 colocalize at mitochondria during apoptosis (Karbowski et al., 2002) and that Bax and pRb interact *in vivo* (Hilgendorf et al., 2013). Therefore, it would be interesting to test the role of Drp1 in pRb-induced apoptosis.

There is increasing evidence that key oncogenes and tumor suppressors modulate mitochondrial dynamics (Boland et al., 2013), which might be significant for tumorigenesis. Therefore, it is possible that regulating mitochondrial dynamics might be a useful therapeutic modality to induce cell death especially in *Rb*-deficient tumors. According to this idea, BIRO1, a cell permeable BH3 peptide, promotes mitochondrial fragmentation in retinoblastoma cells, which leads to cell death (Allaman-Pillet et al., 2015). Understanding how tumor suppressors modulate mitochondrial dynamics could be a major area of research in order to improve cancer treatment.

MATERIALS AND METHODS

Fly stocks

Flies were raised at 25°C on a standard medium. *The UAS-Rbf1* and *vg-Gal4* strains were generous gifts from Joel Silber (Institut Jacques Monod, Université Paris Diderot, Paris, France). The *en-Gal4* and *ptc-gal4* strains were kindly provided by Laurent Théodore (Neuroscience Paris-Saclay Institute, Université Paris Sud, Orsay, France). The *UAS-Debcl* flies were generously provided by Helena Richardson (Research Division, Peter MacCallum Cancer Centre, Melbourne, Australia) (Colussi et al., 2000). The following strains were obtained from the Bloomington Stock Center (Bloomington, IN): $Buffy^{H37}$ (27340), *UAS-Buffy* (32059), $Debcl^{E26}$ (27342), $Debcl^{E26}$ $Buffy^{H37}$ (27338), *UAS-Sod2* (24494), $Sod2^{\Delta 02}$ (27643), $Drp1^{KG03815}$ (13510) and *FLAG-FlAsH-HA-Drp1* (42208). $Buffy^{H37}$, $Debcl^{E26}$, $Sod2^{\Delta 02}$ and $Drp1^{KG03815}$ are null mutations (Sevrioukov et al., 2007; Verstreken et al., 2005). The UAS-RNAi-hep strain (4353R2) was from the National Institute of Genetics stock center (NIG-Fly, Japan). We used a w^{1118} fly stock as the reference strain.

Test of phenotype suppression in the wing

To test the involvement of candidate genes in *Rbf1*-induced apoptosis, the severity of the notched wing phenotype induced by *UAS-Rbf1* overexpression from the *vg-Gal4* driver was assayed in different genetic backgrounds. For each gene, we verified that the alteration of gene expression level (overexpression or mutation) did not induce any wing phenotype. *vg-Gal4>UAS-Rbf1 Drosophila* females were crossed with males bearing a loss-of function mutation for the different genes or allowing their overexpression. The progenies of all crosses were classified according to the number of notches on the wing margin. Wilcoxon tests were performed as described previously (Brun et al., 2002). We considered the difference to be significant when $\alpha<10^{-3}$. To test the implication of *Drp1* in *Debcl*-induced apoptosis, the severity of wing tissue loss induced by *UAS-Debcl* overexpression led by *ptc-Gal4* driver was assayed in different genetic backgrounds. *ptc-Gal4>(UAS-Debcl)$_2$ Drosophila* females were crossed with wild-type males or males bearing a loss-of function mutation for *Drp1*. The distance between L3 and L4 veins was measured perpendicularity to the sixth sensilla of the dorsal row of the anterior wing margin and plotted against the distance between the extremity of veins L4 and L5 for the progenies of all crosses. Student's *t*-tests were performed and results were considered to be significant when $\alpha<5\%$.

TUNEL staining of imaginal discs

Third-instar larvae were dissected in PBS pH 7.6, fixed in PBS with 3.7% formaldehyde, washed three times for 10 min in PBT (1× PBS, 0.5% Triton X-100). Discs were then dissected and TUNEL staining was performed according to the manufacturer's instructions (ApopTag Red *in situ* apoptosis detection kit, Millipore, Temecula, CA, USA). Discs were mounted in CitifluorTM (Biovalley, Marne-La-Vallée, France) and observed with a Leica SPE upright confocal microscope (Leica, Wetzlar, Germany). White patches in the wing pouch (for *Rbf1* experiments) or in *ptc* area (for *Debcl* experiments) were counted for at least 30 wing imaginal discs per genotype. Student's *t*-tests were performed and results were considered to be significant when $\alpha<5\%$.

Immunostaining

Third-instar larvae were dissected in PBS pH 7.6, fixed in PBS with 3.7% formaldehyde. Discs were labeled by overnight incubation at 4°C with anti-

Mmp1 antibody (mouse monoclonal, 1:25, 5H7B11, DSHB, IA) in PBT with FCS (PBS, 0.3% Triton X-100, 10% fetal calf serum). Incubation with anti-mouse-IgG secondary antibody (Alexa-Fluor-488-conjugated goat anti-mouse-IgG (H+L) Antibody, Molecular Probes, Thermo Fisher Scientific, Waltham, MA) or with a Streptavidin Alexa Fluor® 488 conjugate (1:50, Molecular Probes, Thermo Fisher Scientific) was carried in PBT with FCS for 2 h at room temperature. After washing in PBT, wing discs were finally mounted in Citifluor™ (Biovalley) and observed with a Leica SPE upright confocal microscope.

ROS measurement

As described previously (Bergeaud et al., 2013), MitoSOX (Molecular Probes, Thermo Fisher Scientific) was used to measure the mitochondrial production of superoxide. Briefly, 20 wing imaginal discs were dissected in Schneider's *Drosophila* medium (Fisher Bioblock Scientific, Illkirch Graffenstaden, France), then cells were trypsinized. 5 µM MitoSOX were added to the cells, which were incubated at 37°C. Red fluorescence was then measured by flow cytometry by analyzing 2000 events per experimental condition. Flow cytometric measurements were performed using a BD LSRFortessa (Becton Dickinson, Franklin Lakes, NJ). Fluorescence was induced by the yellow–green laser (561 nm). Red fluorescence was collected with a phycoerythrin detector (emission, 578 nm).

RNAs extraction and qRT-PCR

Fifty wing imaginal discs per genotype were dissected on ice in serum-free Schneider medium. Total RNAs were extracted from each sample using the RNeasy Mini kit (QIAGEN), following the manufacturer's instructions. RT was performed on each sample using 4.8 µg of RNA incubated with random primer oligonucleotides (Invitrogen) with Recombinant Taq DNA Polymerase (Invitrogen), according to the manufacturer's instructions.

Real-time PCR analysis was performed using the ABI Prism 7700 HT apparatus (Applied Biosystems). Briefly, PCR was performed with the ABsolute blue qRT-PCR SYBR Green ROX mix (Abgene), using 11 ng of cDNA per RT. Data were normalized against *rp49*. Three independent room temperature experiments were performed and the s.e.m. was calculated from these three independent samples.

Immunoprecipitation

Five third-instar larvae were dissected in PBS pH 7.6, crushed in lysis buffer [Tris-HCl pH 8, 50 mM, NaCl 150 mM, Nonidet P40 1% (NP40), protease inhibitor cocktail (complete Mini EDTA free, Roche, Boulogne-Billancourt, France)]. Cuticles were removed after centrifugation for 10 min at 240 ***g*** at 4°C. An additional centrifugation was performed for 15 min at 6000 ***g*** at 4°C in order to eliminate membrane fragments. The supernatant (total extracts) was recovered and 75 µl were incubated with 15 µl of anti-FLAG antibody attached to agarose beads (Anti-FLAG® M1 Agarose Affinity Gel, Sigma-Aldrich, Saint-Quentin Fallavier, France) overnight at 4°C on a rotating wheel. Immune complexes were then washed five times with lysis buffer and resuspended in loading buffer. Samples were boiled for 5 min and proteins were subjected to western blotting as described below.

Cell fractionation

Ten third-instar larvae were dissected in PBS pH 7.6, crushed in 400 µl of fractionation buffer (Tris-HCl pH 8 10 mM, EDTA 10 mM, sucrose 0.32 M), protease inhibitor cocktail (complete Mini EDTA free, Roche). Cuticles were removed after centrifugation for 5 min at 60 ***g*** at 4°C. 15 µl (total extracts) were kept. An additional centrifugation was realized for 10 min at 2650 ***g*** at 4°C. The supernatant (cytosolic fraction) was recovered. The pellet (mitochondrial fraction) was washed once with fractionation buffer and was then resuspended in 350 µl of fractionation buffer. Samples were boiled for 5 min and proteins were subjected to western blotting as described below.

SDS-PAGE electrophoresis and western blot

Proteins were separated in 4-20% Mini-PROTEAN® TGX Stain-Free™ Precast Gels according to the manufacturer's instructions (BIO-RAD, Hercules, CA) and transferred onto PVDF membrane (Millipore, Darmstadt, Germany). Blots were incubated with primary antibodies [(anti-HA antibody, 1:1000, ab9110, Abcam, Cambridge, UK), anti-Flag.M2 antibody (1:500, Agilent, Santa Clara, CA), anti-Tubulin (1:500, clone B-5-1-2, Sigma) and anti-F1-ATPase (1:1000, β-subunit MS503, MitoScience/Abcam, Cambridge, UK), anti-Tom40 (1:200, Santa Cruz Biotechnology®, Dallas, TX)] overnight at 4°C and were then incubated for 1 h with peroxidase-conjugated anti-mouse-IgG antibody (Jackson ImmunoResearch, West Grove, PA). Immunoreactive bands were detected by Immobilon Chemiluminescent HRP Substrate (Millipore), visualized and quantified using ChemiDoc XRS+ system (BIO-RAD).

In situ proximity ligation assay

ptc>+ and *ptc>Debcl*$_2$ third-instar larvae were dissected in PBS pH 7.6, fixed in PBS with formaldehyde 3.7%, washed three times for 5 min in PBT (PBS, 0.3% Triton X-100). Wing imaginal discs were then dissected and incubated in PBT with FCS (PBS, 0.3% Triton X-100, 10% FCS) at room temperature during 20 min. *In situ* PLA was performed using the Duolink® kit (Olink Bioscience) essentially according to manufacturer's instructions. Briefly, wing imaginal discs were stained with primary antibodies overnight at 4°C. The antibodies used for Duolink assays and their corresponding dilutions are: anti-HA antibody (ab9110, Abcam, 1:200) and anti-DLP1 antibody (BD Transduction Laboratories, 1:200). After washing, wing imaginal discs were incubated with the secondary oligonucleotide-linked antibodies (PLA probes, anti-mouse PLUS and anti-rabbit MINUS) provided in the kit. The oligonucleotides bound to the antibodies were hybridized, ligated, amplified and detected using a fluorescent probe (Detection Kit 563). Discs were mounted in Citifluor™ (Biovalley) and observed with a Leica SP2 upright confocal microscope.

Acknowledgements

We are grateful to Sébastien Szuplewski, Sébastien Gaumer and Frédéric Canal for their critical readings of the manuscript. Confocal microscopy was performed at the CYMAGES imaging facility (University of Versailles/Saint-Quentin-en-Yvelines). We thank Jérôme Estaquier, Mireille Laforge and Nathalie Le Floch for generously providing anti-Drp1 or -Tom40 antibodies. We also acknowledge Vincent Rincheval and Elisabeth Delmas for their help concerning flow cytometry. qRT-PCR experiments were performed in the UMR 1198 'Biologie du Développement et Reproduction' (INRA, Jouy-en-Josas).

Competing interests

The authors declare no competing or financial interests.

Author contributions

I.G. and A.C. designed the study. A.C., V.R. and A.R.-A. performed experiments. All authors analyzed data and wrote the manuscript.

Funding

This research was supported by the Université de Versailles Saint-Quentin-en-Yvelines and the Ecole Pratique des Hautes Etudes (EPHE). A.C. and V.R. were the recipient of a doctoral contract from the UVSQ. A.C. was supported by the EPHE.

Supplementary material

Supplementary material available online at
http://jcs.biologists.org/lookup/suppl/doi:10.1242/jcs.169896/-/DC1

References

Abdelwahid, E., Yokokura, T., Krieser, R. J., Balasundaram, S., Fowle, W. H. and White, K. (2007). Mitochondrial disruption in *Drosophila* apoptosis. *Dev. Cell* **12**, 793-806.

Allaman-Pillet, N., Oberson, A. and Schorderet, D. F. (2015). BIRO1, a cell permeable BH3 peptide, promotes mitochondrial fragmentation and death of retinoblastoma cells. *Mol. Cancer Res.* **13**, 86-97.

Ambrus, A. M., Islam, A. B. M. M. K., Holmes, K. B., Moon, N. S., Lopez-Bigas, N., Benevolenskaya, E. V. and Frolov, M. V. (2013). Loss of dE2F compromises mitochondrial function. *Dev. Cell* **27**, 438-451.

Arnoult, D., Rismanchi, N., Grodet, A., Roberts, R. G., Seeburg, D. P., Estaquier, J., Sheng, M. and Blackstone, C. (2005). Bax/Bak-dependent release of DDP/TIMM8a promotes Drp1-mediated mitochondrial fission and mitoptosis during programmed cell death. *Curr. Biol.* **15**, 2112-2118.

Bergeaud, M., Mathieu, L., Guillaume, A., Moll, U., Mignotte, B., Le Floch, N., Vayssiere, J.-L. and Rincheval, V. (2013). Mitochondrial p53 mediates a

transcription-independent regulation of cell respiration and interacts with the mitochondrial F1F0-ATP synthase. *Cell Cycle* **12**, 2781-2793.
Bertin-Ciftci, J., Barré, B., Le Pen, J., Maillet, L., Couriaud, C., Juin, P. and Braun, F. (2013). pRb/E2F-1-mediated caspase-dependent induction of Noxa amplifies the apoptotic effects of the Bcl-2/Bcl-xL inhibitor ABT-737. *Cell Death Differ.* **20**, 755-764.
Biasoli, D., Kahn, S. A., Cornélio, T. A., Furtado, M., Campanati, L., Chneiweiss, H., Moura-Neto, V. and Borges, H. L. (2013). Retinoblastoma protein regulates the crosstalk between autophagy and apoptosis, and favors glioblastoma resistance to etoposide. *Cell Death Dis.* **4**, e767.
Boland, M. L., Chourasia, A. H. and Macleod, K. F. (2013). Mitochondrial dysfunction in cancer. *Front. Oncol.* **3**, 292.
Bowen, C., Spiegel, S. and Gelmann, E. P. (1998). Radiation-induced apoptosis mediated by retinoblastoma protein. *Cancer Res.* **58**, 3275-3281.
Brachmann, C. B., Jassim, O. W., Wachsmuth, B. D. and Cagan, R. L. (2000). The *Drosophila bcl-2* family member dBorg-1 functions in the apoptotic response to UV-irradiation. *Curr. Biol.* **10**, 547-550.
Bracken, A. P., Ciro, M., Cocito, A. and Helin, K. (2004). E2F target genes: unraveling the biology. *Trends Biochem. Sci.* **29**, 409-417.
Breckenridge, D. G., Stojanovic, M., Marcellus, R. C. and Shore, G. C. (2003). Caspase cleavage product of BAP31 induces mitochondrial fission through endoplasmic reticulum calcium signals, enhancing cytochrome c release to the cytosol. *J. Cell Biol.* **160**, 1115-1127.
Brooks, C., Wei, Q., Feng, L., Dong, G., Tao, Y., Mei, L., Xie, Z.-J. and Dong, Z. (2007). Bak regulates mitochondrial morphology and pathology during apoptosis by interacting with mitofusins. *Proc. Natl. Acad. Sci. USA* **104**, 11649-11654.
Brun, S., Rincheval, V., Gaumer, S., Mignotte, B. and Guenal, I. (2002). reaper and bax initiate two different apoptotic pathways affecting mitochondria and antagonized by bcl-2 in *Drosophila*. *Oncogene* **21**, 6458-6470.
Challa, M., Malladi, S., Pellock, B. J., Dresnek, D., Varadarajan, S., Yin, Y. W., White, K. and Bratton, S. B. (2007). *Drosophila* Omi, a mitochondrial-localized IAP antagonist and proapoptotic serine protease. *EMBO J.* **26**, 3144-3156.
Claveria, C., Caminero, E., Martinez-A, C., Campuzano, S. and Torres, M. (2002). GH3, a novel proapoptotic domain in *Drosophila* Grim, promotes a mitochondrial death pathway. *EMBO J.* **21**, 3327-3336.
Clavier, A., Baillet, A., Rincheval-Arnold, A., Coléno-Costes, A., Lasbleiz, C., Mignotte, B. and Guénal, I. (2014). The pro-apoptotic activity of *Drosophila* Rbf1 involves dE2F2-dependent downregulation of diap1 and buffy mRNA. *Cell Death Dis.* **5**, e1405.
Colin, J., Garibal, J., Clavier, A., Rincheval-Arnold, A., Gaumer, S., Mignotte, B. and Guénal, I. (2014). The *Drosophila* Bcl-2 family protein Debcl is targeted to the proteasome by the beta-TrCP homologue slimb. *Apoptosis* **19**, 1444-1456.
Colussi, P. A., Quinn, L. M., Huang, D. C. S., Coombe, M., Read, S. H., Richardson, H. and Kumar, S. (2000). Debcl, a proapoptotic Bcl-2 homologue, is a component of the *Drosophila melanogaster* cell death machinery. *J. Cell Biol.* **148**, 703-714.
Desagher, S. and Martinou, J.-C. (2000). Mitochondria as the central control point of apoptosis. *Trends Cell Biol.* **10**, 369-377.
Di Fiore, R., D'Anneo, A., Tesoriere, G. and Vento, R. (2013). RB1 in cancer: different mechanisms of RB1 inactivation and alterations of pRb pathway in tumorigenesis. *J. Cell Physiol.* **228**, 1676-1687.
Dorstyn, L., Read, S., Cakouros, D., Huh, J. R., Hay, B. A. and Kumar, S. (2002). The role of cytochrome c in caspase activation in *Drosophila melanogaster* cells. *J. Cell Biol.* **156**, 1089-1098.
Dorstyn, L., Mills, K., Lazebnik, Y. and Kumar, S. (2004). The two cytochrome c species, DC3 and DC4, are not required for caspase activation and apoptosis in *Drosophila* cells. *J. Cell Biol.* **167**, 405-410.
Estaquier, J., Vallette, F., Vayssiere, J.-L. and Mignotte, B. (2012). The mitochondrial pathways of apoptosis. *Adv. Exp. Med. Biol.* **942**, 157-183.
Frank, S., Gaume, B., Bergmann-Leitner, E. S., Leitner, W. W., Robert, E. G., Catez, F., Smith, C. L. and Youle, R. J. (2001). The role of dynamin-related protein 1, a mediator of mitochondrial fission, in apoptosis. *Dev. Cell* **1**, 515-525.
Freel, C. D., Richardson, D. A., Thomenius, M. J., Gan, E. C., Horn, S. R., Olson, M. R. and Kornbluth, S. (2008). Mitochondrial localization of Reaper to promote inhibitors of apoptosis protein degradation conferred by GH3 domain-lipid interactions. *J. Biol. Chem.* **283**, 367-379.
Galindo, K. A., Lu, W.-J., Park, J. H. and Abrams, J. M. (2009). The Bax/Bak ortholog in *Drosophila*, Debcl, exerts limited control over programmed cell death. *Development* **136**, 275-283.
Garcia-Sáez, A. J. (2012). The secrets of the Bcl-2 family. *Cell Death Differ.* **19**, 1733-1740.
Goyal, G., Fell, B., Sarin, A., Youle, R. J. and Sriram, V. (2007). Role of mitochondrial remodeling in programmed cell death in *Drosophila* melanogaster. *Dev. Cell* **12**, 807-816.
Green, D. R., Galluzzi, L. and Kroemer, G. (2014). Metabolic control of cell death. *Science* **345**, 1250256.
Hao, H., Dong, Y., Bowling, M. T., Gomez-Gutierrez, J. G., Zhou, H. S. and McMasters, K. M. (2007). E2F-1 induces melanoma cell apoptosis via PUMA up-regulation and Bax translocation. *BMC Cancer* **7**, 24.
Hardwick, J. M. and Soane, L. (2013). Multiple functions of BCL-2 family proteins. *Cold Spring Harb. Perspect. Biol.* **5**, a008722.
Hershko, T. and Ginsberg, D. (2004). Up-regulation of Bcl-2 homology 3 (BH3)-only proteins by E2F1 mediates apoptosis. *J. Biol. Chem.* **279**, 8627-8634.
Hilgendorf, K. I., Leshchiner, E. S., Nedelcu, S., Maynard, M. A., Calo, E., Ianari, A., Walensky, L. D. and Lees, J. A. (2013). The retinoblastoma protein induces apoptosis directly at the mitochondria. *Genes Dev.* **27**, 1003-1015.
Ianari, A., Natale, T., Calo, E., Ferretti, E., Alesse, E., Screpanti, I., Haigis, K., Gulino, A. and Lees, J. A. (2009). Proapoptotic function of the retinoblastoma tumor suppressor protein. *Cancer Cell* **15**, 184-194.
Igaki, T., Kanuka, H., Inohara, N., Sawamoto, K., Nunez, G., Okano, H. and Miura, M. (2000). Drob-1, a *Drosophila* member of the bcl-2/CED-9 family that promotes cell death. *Proc. Natl. Acad. Sci. USA* **97**, 662-667.
Karbowski, M., Lee, Y.-J., Gaume, B., Jeong, S.-Y., Frank, S., Nechushtan, A., Santel, A., Fuller, M., Smith, C. L. and Youle, R. J. (2002). Spatial and temporal association of Bax with mitochondrial fission sites, Drp1, and Mfn2 during apoptosis. *J. Cell Biol.* **159**, 931-938.
Karbowski, M., Arnoult, D., Chen, H., Chan, D. C., Smith, C. L. and Youle, R. J. (2004). Quantitation of mitochondrial dynamics by photolabeling of individual organelles shows that mitochondrial fusion is blocked during the Bax activation phase of apoptosis. *J. Cell Biol.* **164**, 493-499.
Lin, R., Angelin, A., Da Settimo, F., Martini, C., Taliani, S., Zhu, S. and Wallace, D. C. (2014). Genetic analysis of dTSPO, an outer mitochondrial membrane protein, reveals its functions in apoptosis, longevity, and Aβ42-induced neurodegeneration. *Aging Cell* **13**, 507-518.
Means, J. C., Muro, I. and Clem, R. J. (2006). Lack of involvement of mitochondrial factors in caspase activation in a *Drosophila* cell-free system. *Cell Death Differ.* **13**, 1222-1234.
Mendes, C. S., Arama, E., Brown, S., Scherr, H., Srivastava, M., Bergmann, A., Steller, H. and Mollereau, B. (2006). Cytochrome c-d regulates developmental apoptosis in the *Drosophila* retina. *EMBO Rep.* **7**, 933-939.
Milet, C., Rincheval-Arnold, A., Mignotte, B. and Guénal, I. (2010). The *Drosophila* retinoblastoma protein induces apoptosis in proliferating but not in post-mitotic cells. *Cell Cycle* **9**, 97-103.
Milet, C., Rincheval-Arnold, A., Moriéras, A., Clavier, A., Garrigue, A., Mignotte, B. and Guénal, I. (2014). Mutating RBF can enhance its pro-apoptotic activity and uncovers a new role in tissue homeostasis. *PLoS ONE* **9**, e102902.
Morales, A., Alvarez, A., Arvelo, F., Suárez, A. I., Compagnone, R. S. and Galindo-Castro, I. (2011). The natural diterpene ent-16beta-17alpha-dihydroxykaurane down-regulates Bcl-2 by disruption of the Ap-2alpha/Rb transcription activating complex and induces E2F1 up-regulation in MCF-7 cells. *Apoptosis* **16**, 1245-1252.
Morgenbesser, S. D., Williams, B. O., Jacks, T. and DePinho, R. A. (1994). p53-dependent apoptosis produced by Rb-deficiency in the developing mouse lens. *Nature* **371**, 72-74.
Morishita, J., Kang, M.-J., Fidelin, K. and Ryoo, H. D. (2013). CDK7 regulates the mitochondrial localization of a tail-anchored proapoptotic protein, Hid. *Cell Rep.* **5**, 1481-1488.
Neuspiel, M., Zunino, R., Gangaraju, S., Rippstein, P. and McBride, H. (2005). Activated mitofusin 2 signals mitochondrial fusion, interferes with Bax activation, and reduces susceptibility to radical induced depolarization. *J. Biol. Chem.* **280**, 25060-25070.
Olson, M. R., Holley, C. L., Gan, E. C., Colon-Ramos, D. A., Kaplan, B. and Kornbluth, S. (2003). A GH3-like domain in reaper is required for mitochondrial localization and induction of IAP degradation. *J. Biol. Chem.* **278**, 44758-44768.
Park, J., Choi, H., Min, J.-S., Park, S.-J., Kim, J.-H., Park, H.-J., Kim, B., Chae, J.-I., Yim, M. and Lee, D.-S. (2013). Mitochondrial dynamics modulate the expression of pro-inflammatory mediators in microglial cells. *J. Neurochem.* **127**, 221-232.
Qi, X., Qvit, N., Su, Y.-C. and Mochly-Rosen, D. (2013). A novel Drp1 inhibitor diminishes aberrant mitochondrial fission and neurotoxicity. *J. Cell Sci.* **126**, 789-802.
Quinn, L., Coombe, M., Mills, K., Daish, T., Colussi, P., Kumar, S. and Richardson, H. (2003). Buffy, a *Drosophila* Bcl-2 protein, has anti-apoptotic and cell cycle inhibitory functions. *EMBO J.* **22**, 3568-3579.
Rolland, S. G. and Conradt, B. (2010). New role of the BCL2 family of proteins in the regulation of mitochondrial dynamics. *Curr. Opin. Cell Biol.* **22**, 852-858.
Sandu, C., Ryoo, H. D. and Steller, H. (2010). *Drosophila* IAP antagonists form multimeric complexes to promote cell death. *J. Cell Biol.* **190**, 1039-1052.
Senoo-Matsuda, N., Igaki, T. and Miura, M. (2005). Bax-like protein Drob-1 protects neurons from expanded polyglutamine-induced toxicity in *Drosophila*. *EMBO J.* **24**, 2700-2713.
Sevrioukov, E. A., Burr, J., Huang, E. W., Assi, H. H., Monserrate, J. P., Purves, D. C., Wu, J. N., Song, E. J. and Brachmann, C. B. (2007). *Drosophila* Bcl-2 proteins participate in stress-induced apoptosis, but are not required for normal development. *Genesis* **45**, 184-193.
Sheridan, C., Delivani, P., Cullen, S. P. and Martin, S. J. (2008). Bax- or Bak-induced mitochondrial fission can be uncoupled from cytochrome C release. *Mol. Cell* **31**, 570-585.

Journal of Cell Science

Son, Y., Kim, S., Chung, H.-T. and Pae, H.-O. (2013). Reactive oxygen species in the activation of MAP kinases. *Methods Enzymol.* **528**, 27-48.
Tait, S. W. G. and Green, D. R. (2013). Mitochondrial regulation of cell death. *Cold Spring Harb. Perspect. Biol.* **5**, a008706.
Thomenius, M., Freel, C. D., Horn, S., Krieser, R., Abdelwahid, E., Cannon, R., Balasundaram, S., White, K. and Kornbluth, S. (2011). Mitochondrial fusion is regulated by Reaper to modulate *Drosophila* programmed cell death. *Cell Death Differ.* **18**, 1640-1650.
Tsai, K. Y., Hu, Y., Macleod, K. F., Crowley, D., Yamasaki, L. and Jacks, T. (1998). Mutation of E2F-1 suppresses apoptosis and inappropriate S phase entry and extends survival of Rb-deficient mouse embryos. *Mol. Cell* **2**, 293-304.
Tsubouchi, A., Tsuyama, T., Fujioka, M., Kohda, H., Okamoto-Furuta, K., Aigaki, T. and Uemura, T. (2009). Mitochondrial protein Preli-like is required for development of dendritic arbors and prevents their regression in the *Drosophila* sensory nervous system. *Development* **136**, 3757-3766.
Varkey, J., Chen, P., Jemmerson, R. and Abrams, J. M. (1999). Altered cytochrome c display precedes apoptotic cell death in *Drosophila*. *J. Cell Biol.* **144**, 701-710.
Verstreken, P., Ly, C. V., Venken, K. J. T., Koh, T.-W., Zhou, Y. and Bellen, H. J. (2005). Synaptic mitochondria are critical for mobilization of reserve pool vesicles at *Drosophila* neuromuscular junctions. *Neuron* **47**, 365-378.
Wasiak, S., Zunino, R. and McBride, H. M. (2007). Bax/Bak promote sumoylation of DRP1 and its stable association with mitochondria during apoptotic cell death. *J. Cell Biol.* **177**, 439-450.
Zhang, H., Huang, Q., Ke, N., Matsuyama, S., Hammock, B., Godzik, A. and Reed, J. C. (2000). *Drosophila* pro-apoptotic Bcl-2/Bax homologue reveals evolutionary conservation of cell death mechanisms. *J. Biol. Chem.* **275**, 27303-27306.
Zhao, Y., Tan, J., Zhuang, L., Jiang, X., Liu, E. T. and Yu, Q. (2005). Inhibitors of histone deacetylases target the Rb-E2F1 pathway for apoptosis induction through activation of proapoptotic protein Bim. *Proc. Natl. Acad. Sci. USA* **102**, 16090-16095.
Zimmermann, K. C., Ricci, J.-E., Droin, N. M. and Green, D. R. (2002). The role of ARK in stress-induced apoptosis in *Drosophila* cells. *J. Cell Biol.* **156**, 1077-1087.

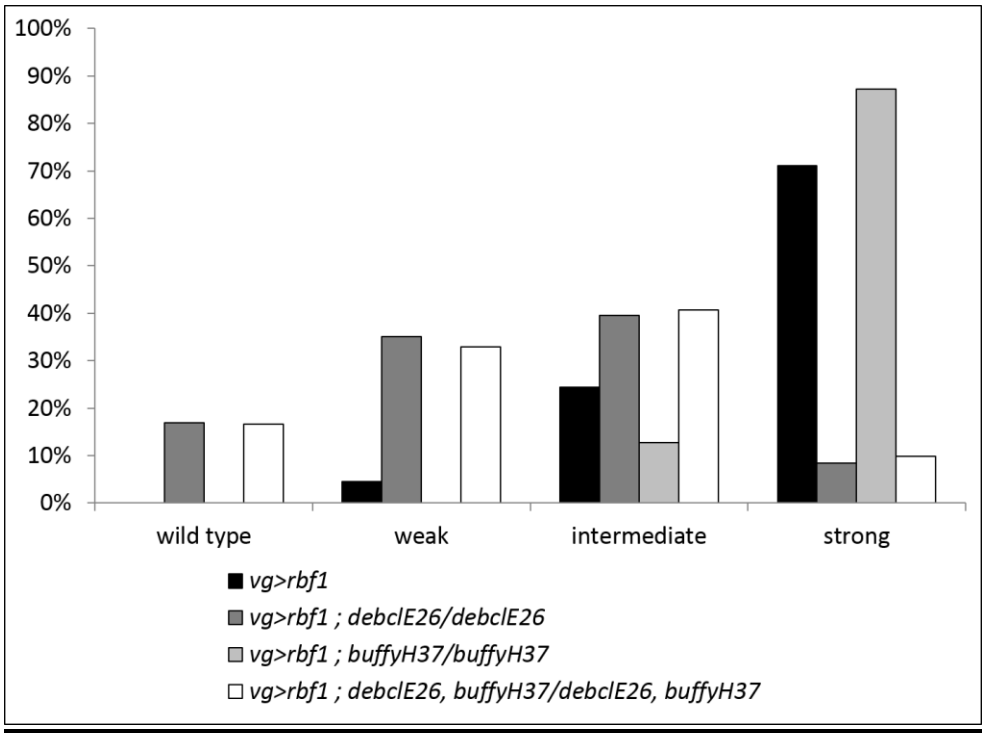

Figure S1: Rbf1-induced *debcl*-dependent loss of tissue.

Distribution of notch wing phenotypes in *vg-Gal4/+ ;UAS-rbf1/+* ; *vg-Gal4/ buffy^{H37} ;UAS-rbf1/+* ; *vg-Gal4/ debcl^{E26} ; UAS-rbf1/+* and *vg-Gal4/ buffy^{H37},debcl^{E26} ;UAS-rbf1/+*. Statistical analysis was performed using Wilcoxon tests: *debcl^{E26}*: n=352, $\alpha<10^{-30}$, Ws=-12,73; *buffy^{H37}*: n=411, $\alpha=2{,}56\ 10^{-5}$, Ws=4,22; *debcl^{E26},buffy^{H37}*: n=380, $\alpha<10^{-30}$, Ws=-12,80. Each experiment was independently performed three times; a representative experiment is shown.

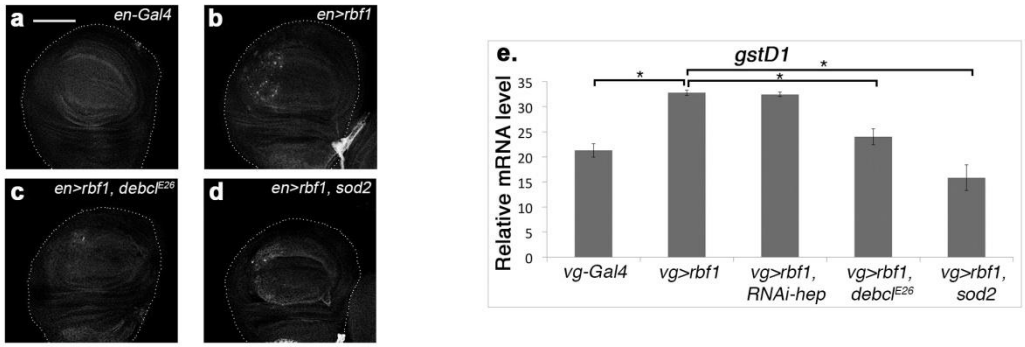

Figure S2: Rbf1 induces JNK activation and ROS production through Debcl.

(a-d) Anti-Mmp1 immunostaining (white dots), of wing imaginal discs from *en-Gal4* (a); *en-Gal4>UAS-rbf1* (b); *en-Gal4>UAS-rbf1,debcl*^{E26} (c) and *en-Gal4>UAS-rbf1,UAS-sod2* (d) larvae. All discs are shown with posterior to the left. Scale bar: 100 µm.

(e) Quantification by RT-qPCR of *gstD1* mRNA in wing imaginal discs from *vg-Gal4*; *vg-Gal4>UAS-rbf1*; *vg-Gal4>UAS-rbf1,UAS-RNAi-hep*; *vg-Gal4>UAS-rbf1,debcl*^{E26} and *vg-Gal4>UAS-rbf1,UAS-sod2* larvae. Data are normalized against *rp49* and the mean of three independent experiments are shown. Error bars are the S.E.M. *: Student's t-test, P<0,05.

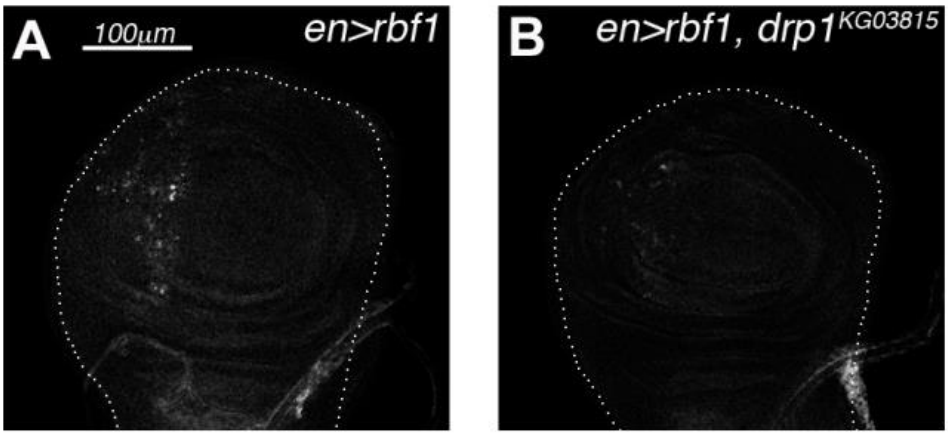

Figure S3: *drp1* is required for rbf1-induced JNK pathway activation.

Anti-Mmp1 immunostaining (white dots), in wing imaginal discs from *en-Gal4>UAS-rbf1* (a) and *en-Gal4>UAS-rbf1,drp1*^{KG03815} (b) larvae. All discs are shown with posterior to the left. Scale bar: 100 µm.